Electron affinities and activation energies for reactions with thermal electrons: SF_6 and SF_5

E. C. M. Chen[1,2,*] and E. S. Chen[2,3]
[1]*University of Houston-Clear Lake, Houston, Texas 77058, USA*
[2]*The Wentworth Foundation, 4039 Drummond, Houston, Texas 77025, USA*
[3]*Baylor College of Medicine, Houston, Texas 77030, USA*
(Received 24 April 2007; published 21 September 2007)

Negative ion mass spectrometry and pulsed discharge electron capture detector data for thermal electron attachment to SF_6 are reported. Electron affinities and activation energies for SF_6 and SF_5 are obtained from these data and literature magnetron, swarm, beam, and collisional ionization data. The thermodynamic and kinetic data cover temperatures from 50 to 7500 K. The largest electron affinity of SF_6, 2.60(10) eV is assigned to the adiabatic electron affinity. The numbers in parentheses indicate uncertainties. Excited state values are (in eV) 2.45(3), 2.20(3), 2.00(3), 1.80(3), 1.60(3), 1.20(3), 1.04(3), 0.80(3), 0.65(3), 0.45(3), 0.35(3), 0.25(3), and 0.10(10). The activation energies range from near zero to 0.65(2) eV. The adiabatic electron affinity of SF_5, 3.85(2) eV and an excited state value, 2.77(5) eV are obtained from a kinetic analysis of published magnetron data. The energies for dissociative electron attachment to give $SF_5(-)$, $F(-)$, and excited state $SF_5(-)$ are 0.20(11) eV, 0.65(10) eV, and 1.28(11) eV from the SF_5-F dissociation energy, the electron affinity of the fluorine atom, and these values. The average relative anion bond orders for the bonding curves is 0.63(2) and for the antibonding curves is 0.30(2). Fourteen Herschbach ionic Morse Person empirical curves are calculated from these data. Six bonding and six antibonding curves are pseudo-two-dimensional cuts through the multidimensional surface. Representative long-range anionic curves are calculated in reaction coordinates analogous to Marcus parabolas.

DOI: 10.1103/PhysRevA.76.032508 PACS number(s): 33.15.Ry, 32.80.Gc, 84.40.Fe

I. INTRODUCTION

In the 1930s the electron affinities (E_a) of atoms were measured using the magnetron (MGN) surface ionization method. In 1949, Teller and Rice noted, "Electron affinities are more difficult to determine and are less accurately known. They are found by a study of the number of negative ions formed under suitable conditions at different temperatures" [1]. Gas phase molecular E_a were not measured until the 1960s [1–10]. Lovelock observed thermal electron reactions in the electron capture detector (ECD) in 1961: $AB+e(-)=AB(-)+E_a$ or $AB+e(-)=A+B(-)+E_1$ [10]. We measured E_a and E_1 with the ECD and negative ion mass spectrometers (NMS) using a kinetic model. Page and co-workers applied the magnetron (MGN) to molecules. Both the ECD and MGN were used to determine E_a of SF_6 and SF_5 in the 1960s [2–10].

At about the same time, Herschbach and Person constructed Morse potentials for six states of $I_2(-)$. The ground state $I_2(-)$ curve crosses the neutral on the "back side" ($r_c < r_e$) similar to Mulliken-Herzberg "c^-" predissociation curves [1,6,11–17]. Herschbach classified negative ion curves based on molecular anion formation or dissociation in a vertical transition, and the signs of $D_e[AB(-)]$, the vertical E_a, (VE_a) and $[E_{dea}=E_a(A \text{ or } B)-D_0(AB)]$, the energy for dissociative electron attachment. The E_{dea} is frequently negative since $E_a(A \text{ or } B)$ is often smaller than the $D_0(AB)$. After replacing the always positive $D_e[AB(-)]$ with E_a we defined $2(2)^3=16$ classes: $M(m)$, $D(m)$, $Mc(m)$, and $Dc(m)$; $m=0-3$, where m is the number of positive metrics. The crossing, $Mc(m)$ and $Dc(m)$ curves are in reaction coordinates analogous to Marcus parabolas. The $M(m)$, $D(m)$ are cuts through the multidimensional surface. These are now called Herschbach ionic Morse Person empirical curves (HIMPEC) [6,11]. In 2004, we predicted the number of positive E_a for a molecule by postulating bonding (b) and antibonding (a) curves in single bond dissociation coordinates. After assigning significantly different E_a to ground and excited states we calculated HIMPEC based on these predictions. Parts of this procedure have been recently applied to O_2, *trans*-azobenzene, Watson Crick adenine/thymine, and nucleic acids [6,13–17].

Sulfur hexafluoride, SF_6, is of fundamental importance since it is the simplest "hexavalent" compound. It is used in the production of semiconductors, as a gaseous dielectric, and as an additive in conducting polymers. However, its global warming potential is thousands of times greater than that of CO_2. It is chemically inert since the D_0(S-F) is large, 4.05(10) eV. The values in parentheses give the combined uncertainties. However, SF_6 is used to characterize electron distributions since it reacts vigorously with thermal electrons. Values of fundamental properties of SF_6 and $SF_6(-)$ have recently been recommended. Despite intense study, the E_{dea}, the adiabatic $E_a(AE_a)$, the number of anion states, and their geometry are uncertain [5–8,18–35].

In 1958, Hickam and Berg calculated the ground state potential for $SF_6(-)$ using an E_a of 1.8 eV estimated from relative bond orders (RBO) [18]. In 1964, Kay and Page reported an $E_a(SF_6)$, 1.5(2) eV using the MGN [26]. In 1968, $E_a(SF_6)>0.7$ eV and $E_1=0.08$ eV were obtained from ECD data [19]. From 1975 to 1985, $E_a(SF_6)$, 0.3–1.0 eV were measured with alkali metal beam and endothermic charge transfer methods giving a "preferred" $E_a(SF_6)$,

*ecmc@houston.rr.com

 ©2007 The American Physical Society

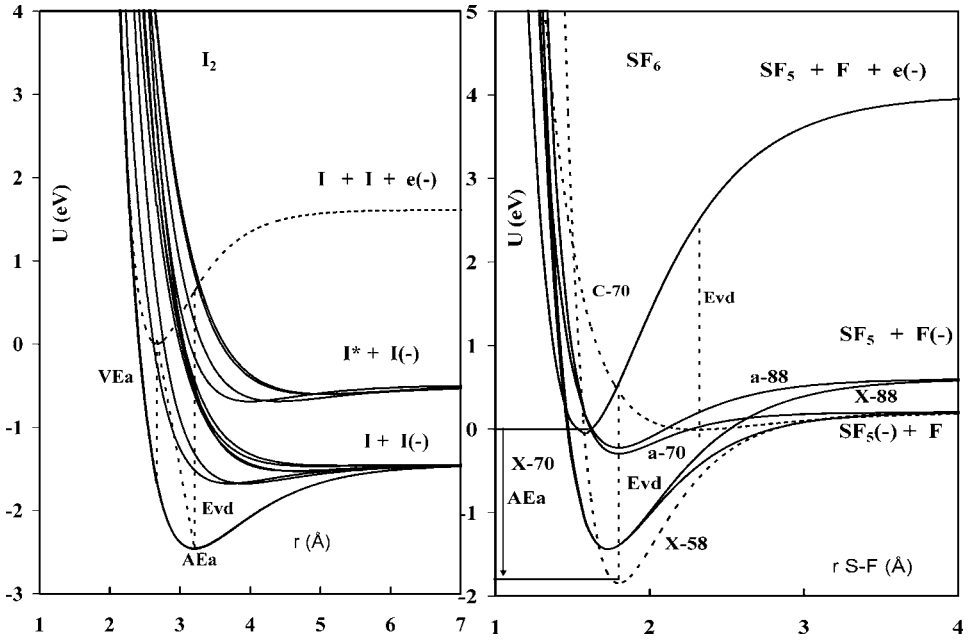

FIG. 1. Ionic and neutral Morse potential energy curves for SF_6 and I_2 to illustrate definitions.

0.6(1) eV. This gave way to the $E_a(SF_6)$, 1.07(6) eV, the weighted average of 1.05(10) eV, 1.15(15), and 1.07(7) eV from ECD, NMS, and thermal charge transfer (TCT) studies. Significantly different values in the National Institute of Standards and Technology (NIST) database are 2.2(2) eV from the photodetachment onset and 0.0(2)–0.8(1) eV from other studies [6–8,23–25,32–36].

The purposes of this article are to (1) report ECD and NMS data from 300 to 635 K; (2) obtain $E_a(SF_6)$ from literature collisional ionization data; (3) revisit magnetron, swarm, and beam data from 50 to 7500 K; (4) obtain electron affinities and activation energies for SF_5 and SF_6 using a least squares procedure and a kinetic model; (5) predict the number of states with positive electron affinities; (6) assign selected $E_a(SF_6)$ to predicted electronic states; (7) calculate relative bond orders from $E_a(SF_6)$ and dissociation limits; and (8) calculate HIMPEC based on experimental data including Franck Condon electron impact ion yield curves.

II. DEFINITIONS

The two types of energy differences between an N electron system plus an electron and its $N+1$ anions are short range E_a (SE_a), with the electrons in the valence shell and long range E_a (LE_a), with repulsions balanced by dipole, quadrupole, or polarization attractions. The LE_a are always positive; by convention E_a are positive for exothermic reactions. The largest E_a or AE_a is an LE_a when all SE_a are negative. For each anion there are three energy differences: E_a in the most stable forms, VE_a in the neutral geometry, and vertical detachment energy (E_{vd}) in the anion geometry. These are illustrated in Fig. 1 for the 12 predicted states of $I_2(-)$ and historical curves for $SF_6(-)$. The former were predicted by the Hund Mulliken rule as described by Teller and Rice. The latter are (year, author, purpose) (a) 1958, Hickam and Berg to illustrate E_a of 1.8 eV by relative bond orders; (b) 1970, Fehsenfeld to explain the $E_1[SF_5(-)]$, 0.43 eV and 0.2 eV; and (c) 1988, Chen and co-workers to include a second dissociation limit [1,6,18–21,32].

III. KINETIC MODEL

The ECD and NIMS studies are concentration jump experiments. A brief pulse of an ultrahigh purity sample is added to a quiescent background and the anion and/or electron concentrations measured as a function of temperature and amount injected. The current in the absence of the sample (I_b), and in its presence (I_{e-}), are continuously recorded and molar response $K[AB]=\{I_b-I_{e-}\}/2I_e$ is calculated. The reactions are

$$AB + e(-) \underset{k_{-1}}{\overset{k_1}{\leftrightarrow}} AB(-) \xrightarrow{k_2} A + B(-), \tag{1}$$

$$e(-) \text{ or } AB(-) + P(+) \xrightarrow{k_D \text{ or } k_N} \text{neutrals}. \tag{2}$$

See below for the rate constants for attachment k_1 and detachment k_{-1} indicated in Eq. (1). With $k_D=k_N=$constant, at steady state

$$K = \frac{k_1(k_N + k_2)}{2[k_D(k_{-1} + k_N + k_2)]}. \tag{3}$$

The equilibrium constant for $AB+e(-)=AB(-)$; $[K_{eq}=k_1/k_{-1}]$ is related to an E_a by

$$\ln K_{eq}T^{3/2} = \ln[Q_{an}] + \ln[S] + 12.43 + \frac{E_a}{RT}. \tag{4}$$

The Q_{an} is the ratio of the anion to neutral partition function and S is the ratio of the spin partition functions. $k_1=A_1T^{-1/2}\exp(-E_1/RT)$, $k_{-1}=A_{-1}T\exp(-E_{-1}/RT)$, and $k_2=A_2T\exp(-E_2/RT)$. The A_i and 12.43 are from fundamental

constants, the translational partition function, and the Debroglie wavelength of the electron.

$$K = \frac{[K_{eq}/2k_D]}{[1/(k_N + k_2) + (K_{eq}/k_1)]}. \quad (5)$$

With fixed intercepts, one point in the limiting positive slope region gives the E_a/R, while one point in the negative slope region gives the E_1/R or $-E_{dea}/R$. Similar equations for the $SF_6(-)$ and $SF_5(-)$ are obtained using the steady state approximation. This model is applicable to the NMS and other swarm and flowing afterglow experiments [6,9,10,13–16,19–21,26–36].

Herschbach ionic Morse Person empirical curves

The acronym HIMPEC gives credit to early work and emphasizes the empirical, not theoretical or experimental nature of the curves. The HIMPEC in reference to $D_e(AB)=0$ are

$$U(AB) = D_e(AB)\{1 - 2\exp[-\beta(r - r_e)] + \exp[-2\beta(r - r_e)]\}, \quad (6)$$

$$U(AB)[-] = D_e(AB)\{1 - 2k_A \exp[-k_B\beta(r - r_e)] + k_R \exp[-2k_B\beta(r - r_e)] - E_a(A,B)\}, \quad (7)$$

$$D_e(AB[-]) = [k_A^2/k_R]D_e(AB), \quad (8)$$

$$r_e(AB[-]) = [\ln(k_R/k_A)]/[k_B\beta(AB)] + r_e(AB), \quad (9)$$

$$\nu_e(AB[-]) = [k_A k_B/k_R^{1/2}]\nu_e(AB), \quad (10)$$

$$VE_a = D_e(AB)(1 + 2k_A - k_R) - E_{dea}. \quad (11)$$

r is the internuclear separation, $r_e=r$ at the minimum of $U(AB)$, $\beta=\nu_e(2\pi^2\mu/D_e[AB])^{1/2}$, and μ is the reduced mass. The E_{dea}, E_a, and VE_a are used to determine dimensionless constants k_A and k_R. Ion distributions, activation energies, anion frequencies, or internuclear distances are used to obtain k_B, which includes the additional mass of the electron [6,11–17].

IV. LITERATURE EXPERIMENTS

In 2004, Christophorou and Olthoff reviewed about 300 studies to suggest properties. No $E_a(SF_5)$ was recommended. Two $D(SF_5\text{-}F)$, 3.9(2) and 4.1(1) eV, and $E_a(SF_6)$, 1.06(6) eV are recommended. Earlier $E_a(SF_6)$ were given as 0.76 eV with a range of 0.0–1.5 eV. The $k_1(300\ K)$, $2.25(5)\times10^{-7}$ cm^3/molecule s, E_1, 0.08 eV are the same as the ECD values [6,7,19]. We reported E_1 from 0 to 0.1 eV and $E_{dea}[SF_5(-)]$, −0.2 eV from NIMS data in agreement with that from the temperature dependence of ion yield curves obtained by Chen and Chantry. However, Fehsenfeld reported $E_{dea}[SF_5(-)]$, −0.43 eV, from flowing afterglow studies [19–21,32–35].

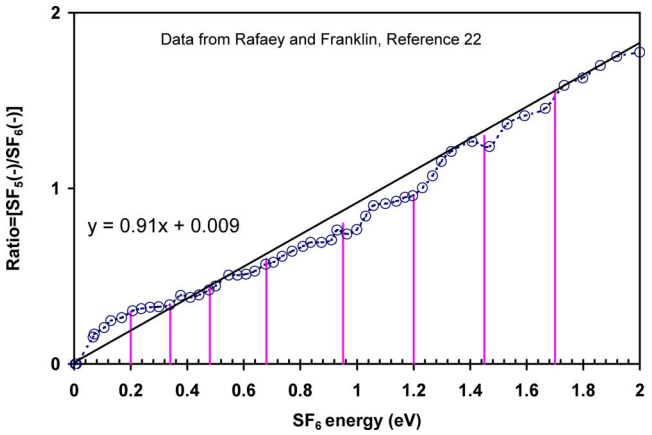

FIG. 2. (Color online) Collisional ionization data for $SF_5(-)$ formation from $SF_6(-)$, Ref. [22]. The equation and line is for a simple linear least squares fit to the data. The vertical lines indicate visual onsets.

The NIST database gives $E_a(SF_6)$, 1.049 eV and $E_a(SF_5)$, 3.800 eV. The complete list gives $E_a(SF_5)$, 2.6(1)–3.8(1) eV and $E_a(SF_6)$, 0.3(1)–2.2(2) eV. The most recent $E_a(SF_6)$, 2.2(2) eV is based on the comment, the E_a, 3.16 eV is the vertical detachment energy. The AE_a is estimated as up to 1 eV smaller." This E_{vd} is from photodetachment data reported by Datskos, Carter and Christophorou, and Grimsrud and co-workers. The literature AE_a is taken as 2.45(20) eV assuming $E_{rr}=0.71$ eV [6–8,24,25]. Rafaey and Franklin reported a succession of thresholds separated by about 0.27 eV in a collisional dissociation study of $SF_6(-)$ as shown by digitized data replotted in Fig. 2. Since the separations are much larger than the vibrational energies in SF_6, they stated "We are unable to give a satisfactory explanation for this regular sequence of thresholds." Also unexplained was their $E_a(SF_6)>1.05$ eV, which is higher than the extant "preferred" 0.54 eV. The onsets can be assigned to electronic states to provide a single experiment giving $E_a(SF_6)$: (in eV) 1.80, 1.53, 1.26, 0.99, 0.72, 0.45, 0.18, and 0.00 with a nominal uncertainty of 0.1 eV [22].

In 1964, Kay and Page reported the $E_a(SF_6)$, 1.5(2) eV from positive slopes in MGN data from 1240 to 1320 K. A more precise method of obtaining E_a was described as follows: "Calculations by Mr. A. L. Farragher, based on the theory of absolute reaction rates indicate that the apparent electron affinity for these six runs is 37(1) kcal/mole," 1.60(5) eV. This procedure was used by Mayer and coworkers and is equivalent to the "fixed intercept" ECD method [2–6,9,10,13,19,26]. In 1968, Malliaris determined the effect of SF_6 on electron concentrations in an ionized argon flow at 7500, 5000, and 3000 K with an SF_6 concentration range of 1000, 0.1–1 atm, reaction time 0.1–1 msec. In these nonequilibrium studies the reaction is quenched and analyzed in a separate region [27]. Shui and co-workers reported the decrease in the effectiveness of electron removal by SF_6 in the CMEF (chemical modeling experimental facility) [29].

In 1973, Spence and Schultz reported that $k_1(SF_6)$ was temperature independent from 300 up to 1200 K in reactions

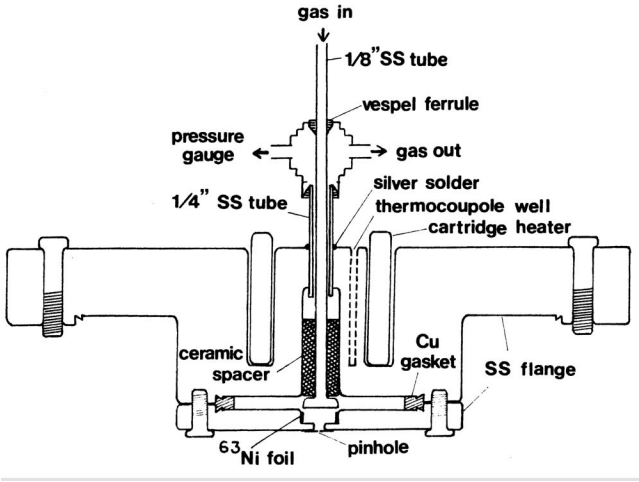

FIG. 3. API ion source used for the data in Refs. [32,34,35].

with 80–100 meV electrons, generated with a retarding potential difference system. However, positive and negative slopes are observed in the data [28]. There are numerous flowing afterglow Langmuir probe studies. The data from Smith *et al.* are chosen to link between the mid and low temperature data [30]. The lowest temperature electron attachment data for SF_6 from 50 to 300 K were obtained by Le Garrec *et al.* using the cinetique de reaction en ecoulement supersonique uniforme (CRESU) device [31].

The experiments are designated chronologically by temperature ranges [19,26–35]. The high temperature (ht) studies are ht-1, magnetron, Kay and Page, Ref. [26]; ht-2, quenched swarm, Mallarias, Ref. [27]; ht-3, electron beam, Spence and Schultz, Ref. [28]; ht-4, CMEF, Shui *et al.*, Ref. [29]. The two low temperature (lt) studies are lt-5, flowing afterglow, Smith *et al.*, Ref. [30] and lt-6, CRESU, Le Garrec *et al.*, Ref. [31]. Our mid temperature (mt) 300–630 K studies are mt-7, ECD, Ref. [19]; mt-8, APIMS, Ref. [32]; mt-9, NMS, Ref. [33]; and mt-10, pulse discharge electron capture detector (PDECD).

Experiment

A custom atmospheric ion source was used to obtain the 1988 data while a commercial chemical ionization mass spectrometer was used for the 1994 data. The API ion source is shown in Fig. 3. The chromatographs and mass spectrometers used in the studies are no longer commercially available, but modern equipment will obtain the same type of data under similar conditions. After stabilizing the temperature, a known amount of SF_6 was injected into and through a chromatographic column, the temperature was changed, and injections repeated. An independent measure of the amount of sample injected in the API experiments was obtained by a parallel chromatographic detector. The carrier gas was argon/10% methane. The temperature was measured by a thermocouple in the ion source. The data were reported as ratios of integrated intensities. Here we report and analyze the data for the individual ions. Additional details can be found in dissertations [32–35].

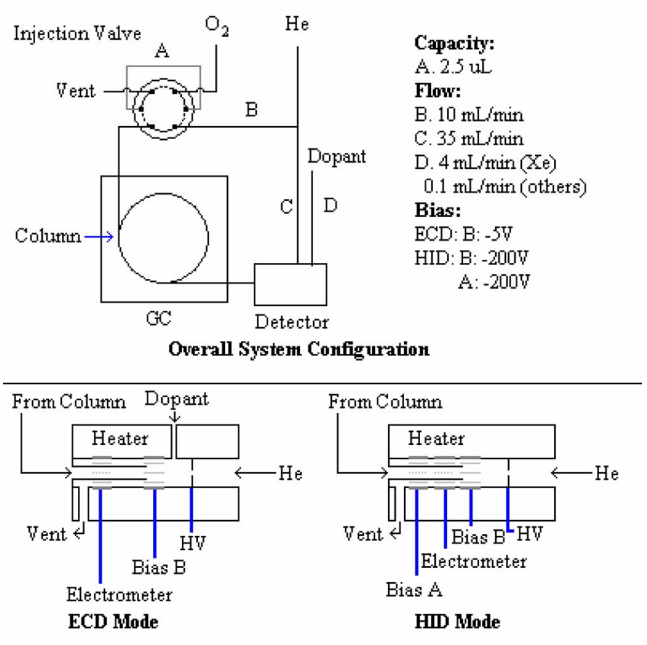

FIG. 4. (Color online) Schematic of pulsed discharge electron capture detector apparatus.

In the commercial instrument, high energy electrons formed by electron impact are rapidly thermalized by H_2 or CO_2 at 0.75 torr. Separate determinations were carried out with different cooling gases. The mass spectra were repetitively collected and intensities of $SF_6(-)$ and $SF_5(-)$ were obtained from sharp peaks [33]. Additional negative ion data obtained using this instrument have been compiled by Stemmler and Hites [36].

Multiple $E_a(O_2)$ predicted by the Hund-Mulliken rule were measured using the PDECD apparatus shown in Fig. 4 [1,14]. This was used for the present studies with a sample of SF_6 diluted in helium. In the PDECD, the 22 eV Hopfield helium emission from a windowless spark discharge generates electrons by ionization of dopants added below the discharge where the sample is introduced. The electrons are thermalized by collisions and collected by applying a small voltage. This is an atmospheric pressure He "flowing afterglow." The purity of the discharge and carrier gas can be checked in the ionization mode.

V. DATA REDUCTION

The positive slope of a standard ECD or NMS plot with only a single linear region is E_a/R and the intercept $11.73+\ln[(Q_{an}*S_{an})(A_N/A_D)]$. The complete ECD curve is calculated from A_1, E_1, E_a, $Q_{an}S_{an}$, $A_D=A_N$, and Eq. (5). The intercepts are defined by $\ln(A_1)=36.84$, from the DeBroglie wavelength of the electron, and $Q_{an}S=1$ [6,14,37]. When the E_a have been measured by another technique, only the E_1 and A_D are completely "unknown." A rigorous least squares procedure including literature values and uncertainties was used to obtain the E_1 and the E_a by iterating through the values in a global nonlinear least squares data analysis as

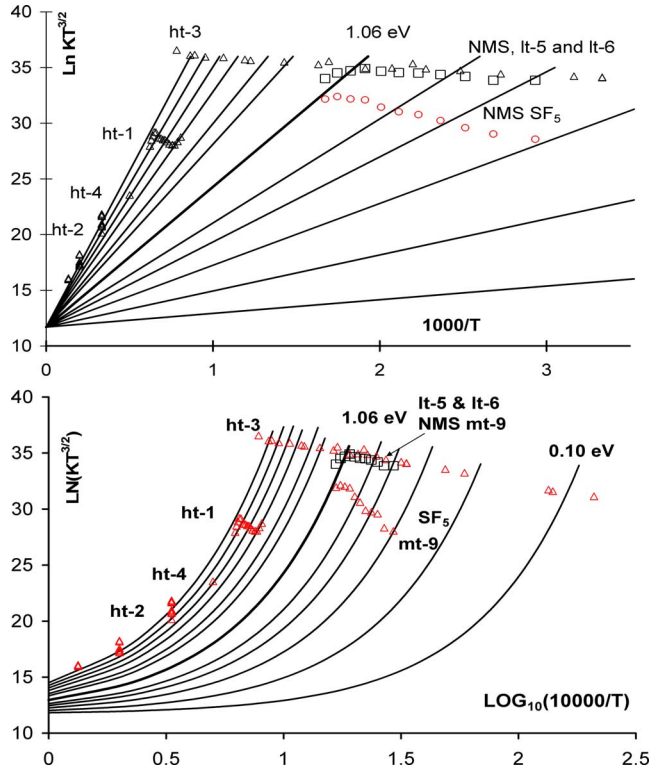

FIG. 5. (Color online). Equilibrium lines calculated using a fixed intercept and the 14 literature E_a given in Table I. The data are taken from the ten experiments discussed above. The data are plotted as $\ln KT^{3/2}$ vs 1000/T (upper) and as $\ln KT^{3/2}$ vs $\log_{10}(10\,000/\mathrm{T})$ (lower) to illustrate the temperature range.

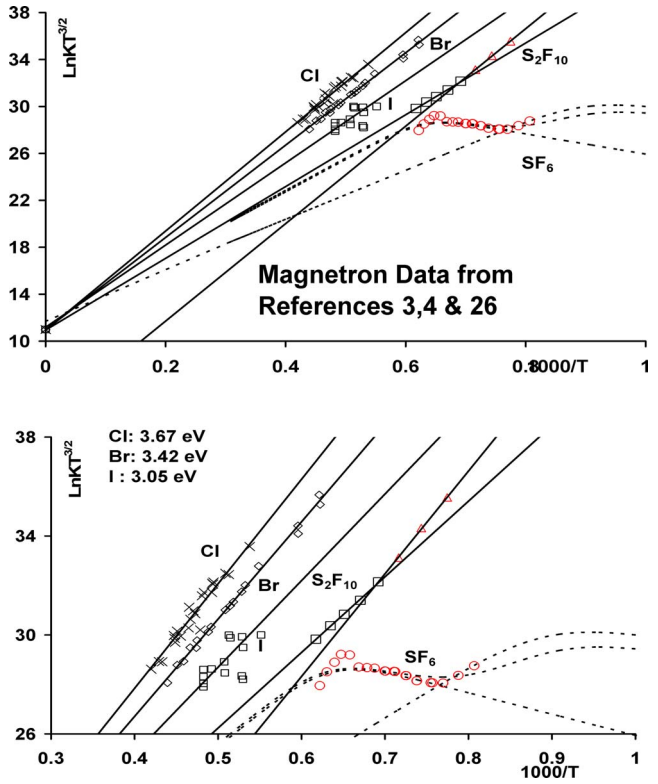

FIG. 6. (Color online) Magnetron data for electron attachment to Cl_2, Br_2, I_2, SF_6, and S_2F_{10} (Refs. [2–5,26]).

described in 1968. These E_1 and E_a are more precise than the most precise single value analogous to improving the precision by averaging values from multiple determinations [14,37].

VI. RESULTS AND DISCUSSION

This section is organized as follows: (a) The number of negative ion states with positive electron affinities are predicted by assuming bonding, antibonding, and X and C states for each dissociation limit and each geometry. For SF_6 this is $2\times3\times2+2=14$ positive E_a for three limits and two geometries. (b) Fourteen literature E_a with uncertainties of about 0.05 eV are selected. (c) Relative bond orders are calculated from these values and E_{dea}. (d) Equilibrium lines calculated for these E_a and experimental data are presented in Fig. 5. (e) The analysis of the MGN, beam, and swarm data is discussed and the results are presented in Figs. 6–9. (f) The analysis of the NMS and ECD data is discussed and the results are presented in Fig. 10. (g) The kinetic and thermodynamic data are summarized in Table I and Fig. 11. (h) Fourteen HIMPEC are presented in Fig. 12.

A. Predicted states and relative bond orders

There are two octahedral geometries for $SF_6(-)$ of concern; those with the SF bond distances of the neutral and those with the SF bond distances of the anion. The three lowest dissociation limits are 0-$[SF_5(-)+F]$, 1-$[SF_5+F(-)]$, and 2-$[SF_5^*(-)+F]$. For each limit there is a bonding (b) and an antibonding (a) curve giving six curves for each geometry or twelve total. Additional curves will arise from spin orbital coupling and dissociations to other excited states of $SF_5(-)$ with negative E_a. The curves are designated 0b0, 1b0, 2b0, 0b1, 1b1, 2b1 and 0a0, 1a0, 2a0, 0a1, 1a1, 2a1, where the first integer represents the dissociation limit and the second the geometry. There are many crossing curves associated

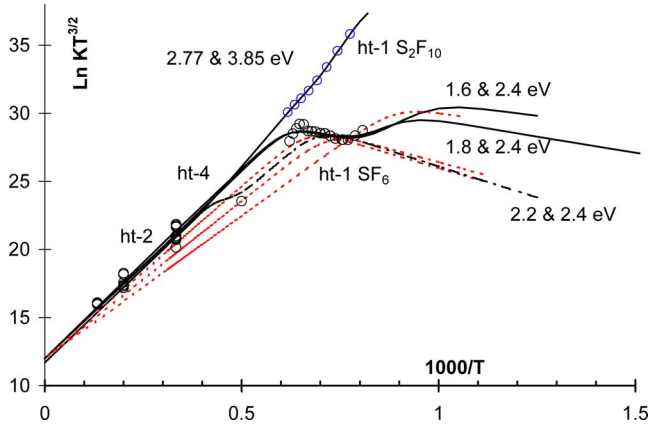

FIG. 7. (Color online) Magnetron and high temperature swarm data for SF_6 and magnetron data for S_2F_{10} from Refs. [26,27,29]. The curves are obtained by fitting the data to Eq. (5).

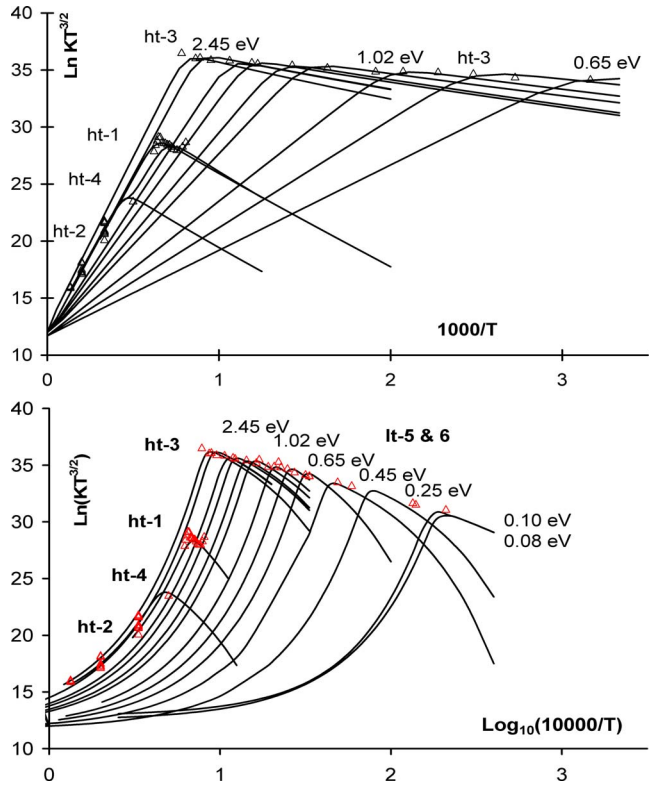

FIG. 8. (Color online) Experimental data for SF_6 plotted as $\ln KT^{3/2}$ vs $1000/T$ (upper) and $\ln KT^{3/2}$ vs $\log_{10}(10\,000/T)$ (lower). The data are from Refs. [26–29]. The curves are the least squares adjusted curves from Eq. (5).

with the X ground state and the C, long-range polarization states. Examples for the 00 limit are $0X0$ and $0C0$. Fourteen positive E_a are selected from the magnetron, photodetachment, collisional ionization, and current best values. These are designated as "literature values" in Table I, with references.

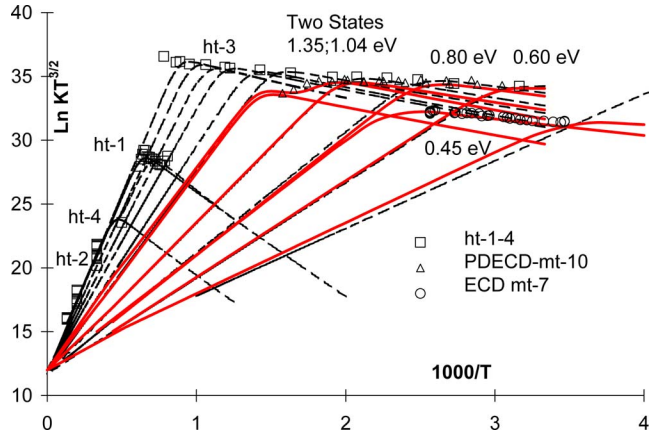

FIG. 9. (Color online) Two sets of PDECD data for SF_6 obtained using the apparatus in Fig. 4. More details can be found in Ref. [14]. The 1968 ECD data were obtained using a tritium foil ECD as reported in Ref. [19]. Also shown are the high temperature data from Refs. [27–30].

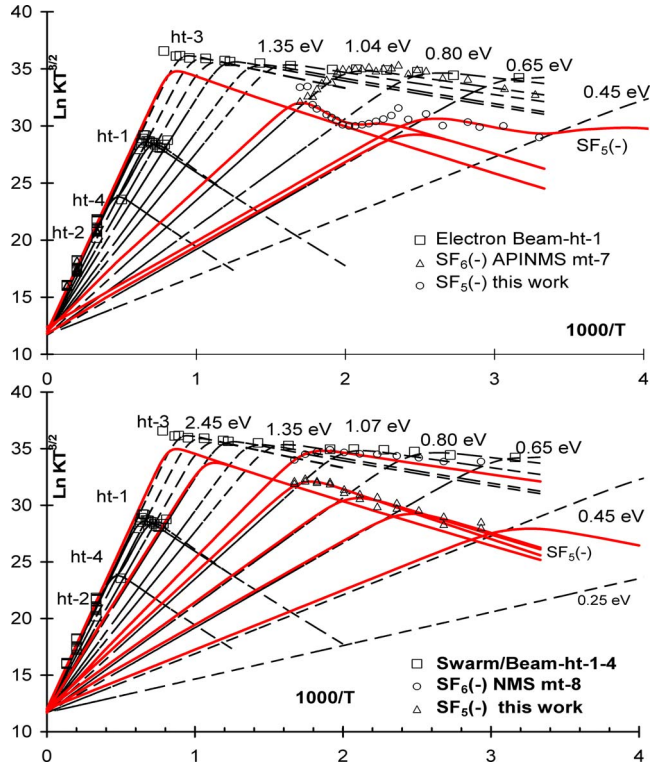

FIG. 10. (Color online) Negative ion mass spectrometry data for $SF_6(-)$ and $SF_5(-)$ obtained in 1988 and 1994. The solid lines are obtained by the least squares fit to these specific data and an equation analogous to Eq. (5) (see Refs. [32–35]).

Following Hickam and Berg, relative bond orders (RBO) are calculated to support the selected values. The experimental RBO for S_2, 0.91 and F_2, 0.77 are larger than the (3/4) and (1/2) predicted by simple molecular orbital theory [6]. The E_{dea} calculated from $E_a(SF_5$, F, and $SF_5^*)$-$D_0(SF_5$-F) are (in eV) [3.85−4.05=−0.20(5)], [3.40−4.05=−0.65(5)], and [2.77−4.05=1.28(10)]. The $E_a(0b0)$, 2.45 eV gives $D[\text{F-SF}_5(-)]/D(\text{SF}_5\text{-F})=2.65/4.05=0.65$; the $E_a(1b0)$, 2.00 eV; $D[\text{SF}_5\text{-F}(-)]/D(\text{SF}_5\text{-F})=2.60/4.05=0.64$; $E_a(2b0)$, 1.4, $D[\text{F-SF}_5^*(-)]/D(\text{SF}_5\text{-F})=2.68/4.05=0.66$. Similarly for the $E_a(0a0, 1a0, 2a0)$ 1.0,0.65,0.25 the RBO are 0.3, 0.3, 0.37. The same procedure for the other geometry gives the RBO shown in Table I. The average RBO for the bonding curves is 0.62(3) while that for the antibonding curves is 0.30(3) comparable to the expected values.

B. Calculation of equilibrium lines

The inclusion of all the literature E_a and E_1 and their uncertainties in a global analysis will require a detailed examination of overlapping values. The E_a in Table I were used with Eq. (4) and a constant intercept to obtain the equilibrium lines shown in Fig. 5. These are predictions of the linear portions of the fit of the experimental data to the kinetic model.

1. Analysis of magnetron data

The NIST tables contain the comment, "The magnetron method, lacking mass analysis, is not considered reliable."

TABLE I. Relative bond orders, electron affinities, and activation energies (in eV).

	E_a (eV) (n=0)	E_1 (eV) (n=0)	E_a (eV), literature	RBO literature	E_a (eV) (n=1)	E_1 (eV) (n=1)	E_a (eV), literature	RBO literature
0*X*0	2.60(10)	0.65(2)	2.45	0.65	2.60(10)	0.65(2)	2.45	0.65
0-*b*-*n*	2.45(3)	0.65(2)	2.45	0.64	2.20	0.63(2)	2.20	0.60
1-*b*-*n*	2.00(3)	0.56(2)	2.00	0.64	1.80	0.43(2)	1.80	0.60
2*b*-*n*	1.60(3)	0.20(2)	1.55	0.69	1.40	0.20(2)	1.26	0.65
References	tw[a]	tw	[8,22,26]	tw	tw	tw	[8,22,26]	tw
0-*a*-*n*	1.03(3)	0.15(1)	1.06	0.31	0.80(3)	0.13(1)	0.72	0.25
1-*a*-*n*	0.65(3)	0.10(1)	0.65	0.30	0.45(3)	0.05(1)	0.45	0.27
2-*a*-*n*	0.25(3)	0.03(1)	0.15	0.37	0.10(3)	0.03(1)	0.10	0.33
0-*C*-*n*	0.10(5)	0.08(1)	0.05	0.06	0.08(5)	0.01(1)	0.05	0.06
References	tw	tw	[6–8,22]	tw	tw	tw	[6–8,22]	tw

[a]This work.

Many of the "direct capture" magnetron E_a from positive slopes have been verified by other methods. We assigned the E_a of cyanocompounds and quinones to ground and excited states as early as 1975. Magnetron data for I_2, Br_2, and Cl_2, from Mayer and co-workers and for S_2F_{10} and SF_6 from Kay and Page are plotted as ln $KT^{3/2}$ vs 1000/T in Fig. 6. The data for S_2F_{10} and SF_6 demonstrate that two or more positive E_a can be measured using the magnetron. Unfortunately, only one set of data for each compound were published. These are plotted in Fig. 7 with other high temperature data [2–5,13,26].

The X_2 were assumed to dissociate to X atoms before electron capture. The E_a(Cl,Br,I)=3.8, 3.6, and 3.2 eV discussed by Teller and Rice in 1949 were obtained from these data and Eq. (4) using $Q_{an}S$ from fundamental constants. Page and co-workers tested their system by measuring E_a(I), 3.18(4) eV from a slope at 1650 K corrected to 0 K. The E_a(Cl,Br,I):3.67(5), 3.42(5), 3.05(10) in eV from a two parameter linear least squares analysis of the data in Fig. 6 are equal to the current NIST, E_a(Cl,Br,I):3.6136, 3.3636, 3.0590 in eV within the random uncertainty. Alternatively, the latter can be used to obtain more precise $Q_{an}S$ [1–6].

Kay and Page obtained $E_a(SF_5)$ from slopes assuming that the dissociation of S_2F_{10} gives SF_5 as in the case of the halogens. Five low temperature slopes were reported (in eV): 3.91, 3.74, 3.91, 3.87, and 3.73 giving the average, 3.83(4) eV. The higher temperature slopes, 2.48, 2.48, 2.49, 2.50, 2.57, average 2.50(4) (in eV) were not definitively assigned. The reproducibility in the slopes, 0.04 eV is much

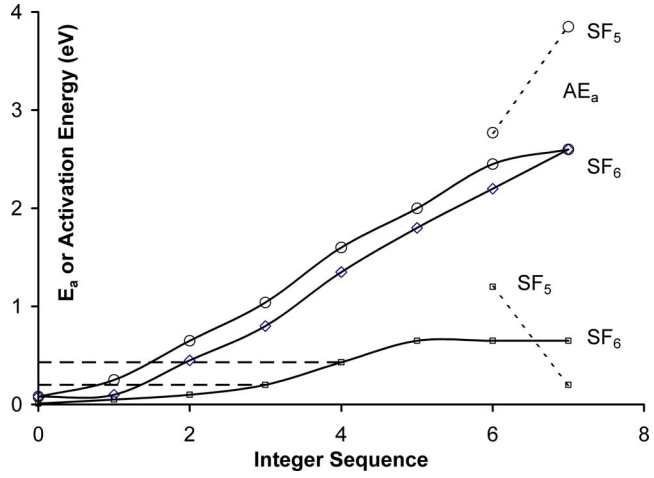

FIG. 11. (Color online) Summary of electron affinities and activation energies for SF_5 and SF_6 in Table I and literature activation energies of 0.43 and 0.2 eV from Refs. [19–21].

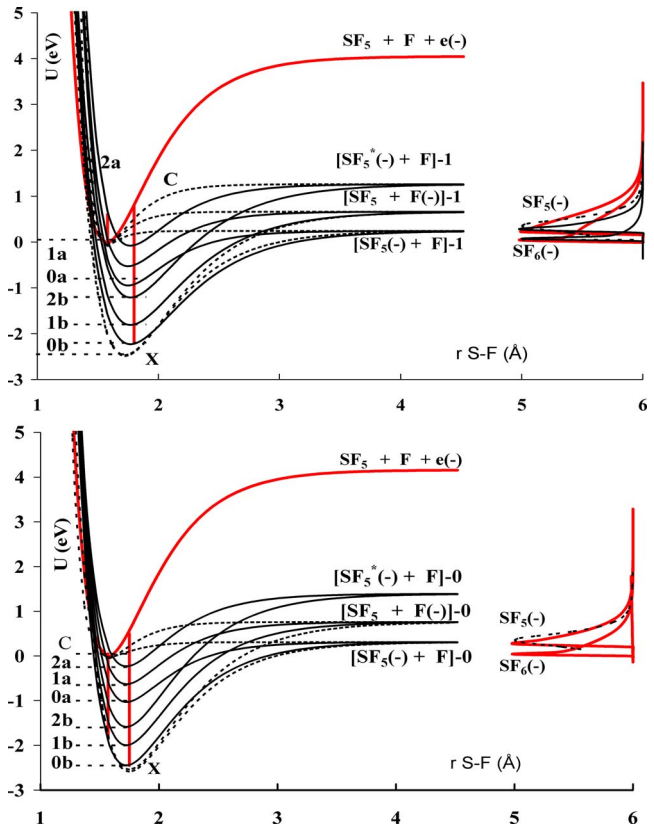

FIG. 12. (Color online). Herschbach ionic Morse Person empirical curves and calculated and experimental ion distributions. The vertical lines are the E_{vd} and the VE_a.

better than that for the $E_a(SF_6)$: (in eV) 1.00, 1.42 1.63, 1.49; 1.88, 1.87 eV, average 1.67(22) eV. We interpret the S_2F_{10} data in terms of two states of $SF_5(-)$ with different $Q_{an}S$. The least squares solution gives intercepts of 10.0(1) and 1.0(1) and $E_a(SF_5^*)$, 2.77(2) eV and $E_a(SF_5)$, 3.85(2) eV as shown in Fig. 7. To our knowledge, this is the only direct measurement of the $E_a(SF_5)$. However, the E_{dea}=−0.20(10) eV combined with the $D_0(SF_6)$=4.05(10) eV gives an $E_a(SF_5)$, 3.85(14) eV [6–8,26].

Kay and Page obtained $E_a(SF_6)$ from positive slopes in the MGN data from 1240 to 1320 K. The slope in the one set of published data gives E_a, 1.80(3) eV, and E_1, 0.33(5) eV. The negative slope between 1320 and 1540 K was attributed to an E_{dea}. We suggest it is a combination of a positive slope and a negative slope as observed in ECD data. This implies a rate constant for ion and electron loss, $k_D=k_N=10^4$ s^{-1} from $K=A_1/k_D$. The calculated curves for additional states E_a, 2.00(4) eV, E_a, 2.20(4) eV, and E_a, 2.45(4) eV with E_1, 0.65(4) eV are shown in Fig. 7. The positive slope above 1540 K was observed to be equal to both the $E_a(F)$ and $E_a(SF_5)$ available at the time. We suggest this could be due to a 1% impurity of S_2F_{10} based on the data in Figs. 6 and 7. The curve for $E_a(SF_6)$, 2.45(4) eV, cuts across the high temperature data [26].

2. Swarm and beam high temperature data

The ht-2 and ht-4 data are plotted with the magnetron data for SF_6 in Fig. 7. The ht-2 data were reported as electron concentration versus amount of SF_6 at 3000, 5000, and 7500 K. The 7500 K plot is linear with concentration giving a constant K_{eq}. The 5000 and 3000 K data are nonlinear giving K_{eq} values that differ by a factor of 5 at 3000 K. The highest data points give an E_a, 2.50(10) eV, E_1, 0.65(5) eV while the lower data points give E_a, 2.00(5), E_1, 0.60(5) eV, and E_a, 2.20(5) eV, E_1, 0.65(5) eV. Shui *et al.* reported "the attachment efficiency of SF_6 is sensitive to the injection temperature; an order of magnitude higher mass flux is required to attach at a fixed axial location when injection is at 3000 K compared to injection at 2000 K." The ht-4 2000 K data gives an E_a, 2.20(5) eV, and E_1, 0.65(5) eV and helps define the E_1. The ht-4 3000 K values are from two concentrations. The values support E_a, 2.50(5) eV, E_1, 0.65(5) eV, E_a 2.00(5), E_1, 0.60(5) eV, and E_a, 2.20 eV, E_1, 0.65(5) eV from the other data [27,29].

The 1973 electron beam data are frequently cited to show that the $k_1(SF_6)$ is temperature independent and that A_1 for the electron attachment approaches a common limit. All the high temperature data are plotted in Fig. 8. Spence and Shultz noted, "In a swarm experiment, the $SF_6(-)$ ions make many collisions, making stabilization possible. In a beam experiment there are essentially no such collisions." The initially formed excited anion state is stabilized by internal vibrational relaxation, which is the source of the lower apparent activation energy for these data.

The four sets of high temperature data give $E_a(SF_6)$, 0.65(5) eV to 2.60(10) eV with E_1 from 0.20 to 0.10 eV. In Fig. 8 the least squares calculated curves are shown as $\ln KT^{3/2}$ vs 1000/T. Additional E_a from 0.08 to 0.65 eV and E_1 from 0.10 eV to near zero are obtained from the lt-5 and lt-6 data. The set of curves covering the complete temperature range are shown as $\ln KT^{3/2}$ vs $\log_{10}(10\,000/T)$ in Fig. 8. The curves in Fig. 8 can be compared to the predicted curves in Fig. 5.

C. ECD, PDECD, and NMS data

Since 1968, we have carried out many ECD and NMS determinations for SF_6 to establish the validity of experimental data. The temperature dependence of the intensity and the ratio of $SF_5(-)/SF_6(-)$ was routinely measured to determine the electron energy distribution. Also determined is the magnitude of the k_D and hence the "cleanliness" of the system. In order to obtain an E_a, a positive slope in the $\ln KT^{3/2}$ vs 1000/T plot must be observed. In Fig. 9 the 1968 ECD data and two sets of PDECD data are plotted. The dotted lines are the curves shown in Fig. 8. The solid curves are obtained from the ECD and PDECD data. The E_a are 1.04(1), 0.80(1), 0.65(1), 0.45(1), and E_1 0.13(1), 0.11(1), 0.10(1), and 0.08 (all in eV). A two state curve was constructed to show the transition between the 1.04 and 1.35 eV values.

In 1988, the $SF_5(-)/SF_6(-)$ ratio was reported from ion intensities measured using the API source shown in Fig. 3. No F(−) was observed establishing $E_a(SF_5)>E_a(F)$, 3.40 eV. This gave the $D_0[F\text{-}SF_5(-)]$, 1.35(15) eV or an $E_a(SF_6)$, 1.15(15) eV from E_{dea}, −0.20(5) eV. A value of $E_a(SF_5)$, 3.85(15) eV was obtained from the S-F dissociation energy, 4.05(10) eV. In 1994, an E_a, 1.07(7) eV was obtained from positive slopes in ECD and NMS $SF_6(-)$ data. With the same instrument, the E_a(nitrobenzene) was determined to be 1.00(6) eV in agreement with an ECD value of 1.00(2) eV. The current E_a(nitrobenzene) is 1.00(1) eV in NIST [6–8,13,32–36].

The API NMS and the chemical ionization NMS data for $SF_6(-)$ and $SF_5(-)$ are plotted in Fig. 10. The $E_a(SF_6)$ obtained from these data are (in eV) 1.07(1), 0.80(1), 0.65(1), 0.45(10) with E_1 from 0.08 to 0.20 eV. The API data for $SF_5(-)$ are fit to two state curves since additional structure is observed. This may be to vibronic interactions. Such assignments are beyond the scope of this paper. The chemical ionization $SF_5(-)$ data are fit to single state curves, since there is much less structure. This could be due to the lower pressure in the ion source or due to use of intensities from sharp peaks rather than the integrated area over broad peaks as used in the API MS data. The data for the formation of $SF_5(-)$ can be extrapolated to higher temperatures using the kinetic model. Single state curves are constructed with an E_a, 1.8 eV and E_1, 0.32 eV and E_a, 2.45 eV and E_1, 0.32 eV to overlap the lower temperature data point. Thus, both dissociative and nondissociative electron capture occur in the electron beam experiment. This supports the AE_a obtained from the high temperature data and opens the possibility of an even higher AE_a based on the last two electron beam data points. The $E_a(SF_6)$ from the two sets of $SF_5(-)$ data are consistent with each other and the values obtained from the other techniques. The E_{dea}, −0.25(10) eV combined with the magnetron $E_a(SF_5)$, 3.85(2) eV gives the $D_0(SF_5\text{-}F)$=4.10(10) eV.

D. Summary of the experimental results

The new results are summarized in Table I and in Fig. 11. The E_a from this study agree with the selected E_a in Table I. The E_a from 2.60 to 0.10 eV determined by multiple techniques are accurate and precise. The random uncertainties are all less than 5 meV. Systematic uncertainties of 0.03 eV are estimated for the values from 2.45(3) to 0.25(3) eV and are larger at the extremes 2.60(10) and 0.10(5). The $AE_a(SF_6)$ must be less than the $AE_a(SF_5)$, $AE_a(F)$, and the experimental vertical detachment energy, 3.16(20) eV. The experimental values of the E_a give reasonable relative bond orders.

The E_a and E_1 are plotted sequentially in Fig. 11. The "0" values are *LEa*; the "1–3" values are antibonding states, the "4–6" values are bonding states, and the "7" value is the AE_a. The two curves are for the two geometries. The $AE_a(SF_6)$ is slightly larger than the $E_a(0b0)$ since the "0" geometry is that of the octahedral anion. The ions in the neutral geometry are separated from the ions in the anion geometry by about 0.20 eV. This is similar to the separations between collisional onsets observed by Rafaey and Franklin. There is a change in the E_1 at the $E_a > 1.06$ eV as shown in Fig. 11.

The E_1, 0.65(1) eV for the bonding states is like a "c^-" "back side crossing" predissociation curve for diatomic molecules described by Mulliken [12]. The activation energies for the antibonding states for $SF_6(-)$ are less than 0.2 eV consistent with the formation of the parent negative ion at low energies. The two $-E_{dea}$ reported in the literature 0.20(5) eV and 0.43(5) eV are shown as limits to E_1. Using the literature dissociation energy of 4.05(10) eV and the electron affinity of F, 3.4012 eV, the energies for the formation of $SF_5(-)$, F(−), and excited state $SF_5(-)$ from SF_6 are 0.20(11) eV, 0.65(10) eV, and 1.28(11) eV.

E. Herschbach ionic Morse Person empirical curves

The HIMPEC, and experimental and calculated ion distributions for $SF_6(-)$ and $SF_5(-)$ are shown in Fig. 12. In order to calculate HIMPEC, the dissociation limits, the neutral Morse parameters and three points on each curve are required. The neutral parameters used for the HIMPEC are $D_0=4.05$ eV, $r_e=156$ nm, ν, 948 cm^{-1} [7]. The $-E_{dea}$ from the $D_0(SF_6)$ $-E_a(SF_5^*, SF_5, \text{and F})$ are given above: 0-[0.2 eV], 1-[0.65 eV], and 2-[1.28 eV]. The *C* curves are obtained using the neutral r_e. The *X* curves are calculated with the anion $r_e=172$ pm to give the AE_a. These are only representative of the multitude of curves in reaction coordinates. The *X* and *C* curves are $Mc(2)$ since only the E_{dea} is negative.

The E_a provides one point and the E_1 another point on each curve. The $0b1$ and $0b0$ curves give $E_{vd}<3.17$ eV. The other *b* curves give backside crossings from 0.3 to 0.65 eV. All of the *a* curves are consistent with a zero energy peak for $SF_6(-)$. The $2a1$ and $2a0$ curves are $M(1)$ and give the calculated distribution for $SF_5(-)$ as seen in Fig. 12. The other *a* curves cross the neutral below the $v=1$ levels and give activation energies between 0 and 0.1 eV. These curves and the *b* curves are $M(2)$ with only E_{dea} negative. These HIMPEC are good first approximations to the pseudo one dimensional curves.

A superficial examination of the published data indicates no major inconsistencies in experimental and theoretical $E_a(SF_6)$ as will be discussed in the Appendix. However, only the values in Table I have been critically evaluated and included in the global least squares. Therefore the dimensionless constants and anion parameters used to calculate the curves are not presented. A major possible change could be the identification of a larger E_a, which would then become the AE_a. However, the largest possible AE_a is the experimental E_{vd}, 3.16(20) eV.

VII. CONCLUSIONS

The major conclusions of this paper dealing with the subject molecules are (1) The number of anion states of SF_6 can be predicted for two geometries and three single bond dissociation channels. (2) The E_a and E_1 reported in Table I support these predictions and other experimental E_a. (3) The E_a agree with predicted relative anion bond orders. (4) The activation energies range from near zero to 0.65 eV indicating crossings at $v=0,1,2$ on the "front side" and up to $v=8$ on the "back side." (5) Multiple $E_a(SF_6)$ can be identified in magnetron, electron beam, electron swarm, ECD, NMS, and collisional ionization data. (6) The $E_a(SF_5)$ and $E_{dea}[SF_5(-)]$ determined from the magnetron method are consistent with literature values. (7) The Herschbach ionic Morse Person empirical curves account for previously conflicting observations and agree with ion yield curves.

Some of the specific conclusions for the subject molecules can be generalized: (I) The number of positive electron affinities can be predicted from single bond dissociation channels. (II) The largest accurate and precise electron affinity can be assigned to the adiabatic electron affinity and lower values to excited states. (III) Systematic uncertainties due to interpretations can be identified in reported values. (IV) The calculation of relative bond orders can be used to support experimental and/or theoretical electron affinities. (V) Herschbach ionic Morse Person empirical curves provide a convenient technique of consolidating data from different experiments. A protocol for these procedures is given in the Appendix.

ACKNOWLEDGMENTS

The work was supported by the Wentworth Foundation, Inc. Figure 4 is taken from an unpublished communication by C. Herder. He also proposed an ideal universal electron capture detector (IUECD) to cover a wide range of temperature, pressure, and concentrations based on the devices used to obtain the data described in this paper.

APPENDIX

This appendix provides additional references ([38] forward) so that the general audience can better follow the specific arguments of the paper. It discusses the statistical tools

used to evaluate and assign the E_a for SF_5 and SF_6 and relates these to recent similar evaluations for O_2, CS_2, C_6F_6, the nucleic acids, *trans*-azobenzene, and anthracene. Nitrobenzene is used as a reference point since its adiabatic electron affinity (AE_a) has remained constant since 1955 [6,8,13–17,37]. The earliest reviews of gas phase electron affinities (E_a) are in monographs by Massey [38]. In 1953, Pritchard evaluated the extant E_a [39]. Beginning in the 1940s, relative E_a were obtained from reduction potentials (ERD) and the Nernst equation: $E_a(A)-E_a(B)=\mathrm{ERD}(A)-\mathrm{ERD}(B)$ assuming equal solution energy differences as discussed by Streitweiser in 1960 [40]. The use of ERD and donor acceptor complex energies to obtain absolute electron affinities by scaling to gas phase values was summarized by Briegleb in 1963 [41].

The gas phase methods of measuring E_a are classified as equilibrium, beam, and photon methods. The electron capture detector (ECD), magnetron (MGN), negative ion mass spectrometry (NMS), and swarm equilibrium methods obtain E_a from measurements of the equilibrium constant for thermal electron reactions at different temperatures. These values are "absolute" since they are obtained from experimental data and fundamental constants [1–10]. The equilibrium thermal charge transfer (TCT) data, like the reduction potential data, give relative E_a which must be calibrated to absolute values. The thresholds for reactions with electron or alkali metal beams (AMB) are combined with bond dissociation energies or ionization potentials to obtain E_a. Photon methods, photodetachment, or anion photoelectron spectroscopy give E_a from electron onsets and the photon energy. In 1983, the experimental, theoretical, and semiempirical methods used to obtain electron affinities were summarized and a comprehensive but unevaluated list of the E_a of atoms, radicals, and molecules obtained using these methods up to 1981 was prepared. Specific reviews are available for the EB, TCT, AMB, and photon studies [42–46].

In 1988, Chen and Wentworth (a) evaluated the E_a of organic molecules, (b) obtained E_a from empirical substitution and replacement rules, and (c) classified molecules to obtain E_a from reduction potentials. In 1991, reduction potentials of the nucleic acids were measured and the E_a obtained by calibrating to the gas phase electron affinities of acridine and anthracene. The AE_a of acridine and anthracene are now about 0.15 eV higher giving E_a: (in eV) adenine, 1.09(5), guanine, 1.60(10); cytosine, 0.70(5), uracil, 0.94(5), and thymine, 0.93(5). In 1999, the electron affinities of over 150 organic molecules were obtained from reduction potentials [47–49].

Both precision and accuracy are characteristics of the measurement procedure, not the value. In 1988, we estimated the total uncertainties in various methods: (in eV) ECD, 0.05; MGN, 0.20; AMB, 0.15; and TCT, 0.10. The uncertainty is now reduced to 0.10 eV for the absolute magnetron method by eliminating bias errors [1–5,26,47]. Random errors are established by multiple determinations. In order to evaluate bias errors, the same quantity must be measured by at least two different procedures. Ideally, the two procedures give the same value within the mutual uncertainties. Then, the weighted average is the "best" value. It is calculated from the equations: $y(\mathrm{avg})=\Sigma(w_i y_i)/[\Sigma(w_i)]$, $w_i=1/s_i^2$, and $s^2_{y\ \mathrm{avg}}=1/[\Sigma(w_i)]$, where the individual values are the y_i and the uncertainties in the y_i are the s_i. If the values do not agree within the random errors, then a systematic error between the two methods can be inferred. Uncertainties should not be given to more than two figures.

In 2004, we evaluated over 300 molecular E_a in the National Institute of Standards and Technology (NIST) website. For nitrobenzene, the five E_a determined using different methods are (in eV) 1.00(1), anion photoelectron spectroscopy; 1.01(10), TCT; 1.00(6), NMS; 1.02(5) TCT; and 1.00(2), ECD. The weighted average is 1.005(9) eV. Note that the uncertainty in the weighted average is smaller than the smallest individual uncertainty. In the same manner, when experimental E_a or activation energies and their uncertainties are included in a global nonlinear least squares analysis of the combined data, as was done for SF_5 and SF_6, the random uncertainty in the resultant values will not be degraded [8,13,37].

The agreement for the above methods suggests that the methods contain no systematic uncertainties. Thus any significantly different values obtained from these methods must be explained as in the case of SF_6. The $E_a(SF_6)$ in NIST clustered around five values in 2004. The weighted average of the overlapping values (in eV) 0.95(50), 1.07(7); 1.15(15), 1.05(10), and 1.4(4), is 1.07(6). It was assigned to the AE_a, and the lower values 0.75(10), 0.52(5), and 0.32(15) were assigned to excited states. The photodetachment onset 3.2(2) eV implied a 2.09 eV rearrangement energy. Upon noting the multiple onsets observed by Refaey and Franklin, an AE_a above 2.2 eV was postulated from the comment in NIST "the 3.16 eV is a vertical detachment energy; the AE_a is estimated as up to 1 eV smaller." This was combined with the multiple onsets, the relative bond orders, and the analysis of the high temperature data to give the $AE_a(SF_6)$, 2.60(10) eV. Lower values were assigned to the positive E_a predicted by single bond dissociation channels [6–8,22,26–29].

We analyzed anion photoelectron spectra published in the literature to obtain AE_a (in eV): *trans*-azobenzene, 1.40(2); C_6F_6, 1.3(1); adenine, 1.08(5); cytosine, 1.043(5); uracil, 0.96(2); thymine, 0.93(2); O_2, 1.07(2); CS_2, 0.90(10); and anthracene, 0.70(2). These are confirmed by ECD studies and/or reduction potentials [8,13–17,40–42]. They are equal to the weighted average of the largest values in NIST: (in eV) O_2, 1.10(7); CS_2, 0.90(10); anthracene, 0.66(6); and C_6F_6, 1.26(7). When searching NIST for compounds containing given elements, a single unevaluated value without errors is returned: (in eV) O_2, 0.448; CS_2, 0.512; anthracene, 0.530(5); C_6F_6 0.520; adenine, 0.012; thymine, 0.069; and uracil, 0.086. The values for cytosine found in a search by name are 0.0850(80) and 0.2300(80). These are all for excited states. Only two values in NIST were not assigned to the AE_a since they contained a systematic uncertainty. The E_a(biphenylene), 0.890 eV (#117 from a CH search), is probably for an isomer, acenaphthylene, AE_a, 0.90 eV; E_a, 0.7,0.6, and 0.5 eV determined using ECD and ERD methods. The E_a(*t*-amyl-nitrobenzene), 2.168 eV (#168 from a CHON search) was incorrectly calibrated to E_a(nitrobenzene), 2.1 eV. The value should be about 1 eV.

No E_a for guanine or *trans*-azobenzene are in NIST. We identified the AE_a and E_a of trans-azobenzene in anion photoelectron spectra. The excited state E_a were measured in ECD and TCT studies while the AE_a was measured in electron transfer dissociation and Marcus electron transfer studies. The AE_a and excited state E_a were measured sequentially in reduction potential studies. Based on the AE_a the E_a (cytosine), 0.70(5) eV from ERD, was assigned to an excited state. Other reduction potentials of *C*, *U*, and *T* are equal within 0.1 eV in agreement with the AE_a. Thus excited state E_a can be obtained from reduction potential data [6,9,13–17,50].

Based on the similarity of the procedure for the assignments for these molecules and SF_6, a general protocol can be described. The first step is to compile all of the reported values, including those from reduction potentials. Then the weighted averages of values are calculated. If all of the values overlap, as in the case of nitrobenzene, the best estimate of the AE_a is the weighted average. If there are significantly different values then the largest weighted average is the AE_a. Next, the number of positive valence state E_a is predicted. For O_2, the Hund Mulliken rule predicts 54 total states from $O(^3P)+O(-)(^2P)$ to be 6 $O(-)(^2P)\times 9$ $O(^3P)=54$. This gives 27 bonding spin orbital coupling states with positive E_a not considering right (left) symmetry. These have been measured by ECD, anion photoelectron spectra, and other methods. The XY_2 Walsh diagrams predict two anion states for CS_2. The E_a observed in both ECD and photon experiments 0.53(5) eV and 0.90(10) eV are assigned to the linear and bent ions, respectively. For larger molecules the predictions are more difficult. In anthracene, two fourfold and one twofold positive E_a are predicted from the three types of C-H single bonds. Three E_a, 0.530(5), 0.65(1), and 0.70(1) eV have been identified using two or more methods. By analog to SF_6 12 positive E_a are postulated for C_6F_6, from three low lying channels and two geometries. In *trans*-azobenzene, there are *cis* and *trans* isomers and different types of C-H bonds in each isomer while in cytosine, besides the tautomers, there are geometric changes [6,13–16].

The complexity of determining the electronic states for polyatomic molecules (anions) is described by Herzberg on page 7 of the third volume in his trilogy [51]. "Every electronic state of a polyatomic molecule is characterized by a $3N$-6 dimensional hypersurface. If the potential surface has no minimum, the electronic state is unstable; if the potential surface has at least one minimum, the electronic state is stable. There may be large differences in these potential surfaces for different electronic states […]. Potential surfaces with several minima occur not infrequently (sometimes corresponding to different isomers) […]. Even in the simplest case, that of a triatomic molecule, the potential surface is three dimensional in a four dimensional space" (for nonlinear molecules) [51].

Once the significantly different values from all sources including reduction potentials have been identified and assigned to predicted states, other data can be used to construct Herschbach ionic Morse Person empirical curves as we have done for C_6F_6, CCl_4, C_6H_6, SF_6, I_2, Br_2, Cl_2, F_2, and O_2. Note that only for the diatomic molecules has spin orbital coupling been considered. For SF_6, there must be additional dissociation channels leading to excited states of $SF_5(-)+F$ or $SF_5+F(-)$ to account for the ions observed above two electron volts electron impact energy since the spin orbital coupling values for S and F are small [6,11–16].

In summary, the results for SF_6 obtained using this protocol remove many perceived conflicts. However, there are still questions concerning the multidimensional surface representing the reactions of electrons with SF_6 and with molecules in general. A specific shortcoming is the knowledge of the number and values of the energies of the electronic states of anions. We note that in spite of many studies since 1994, no new $E_a(SF_6)$ have been previously reported. This paper joins Herzberg in observing that "potential surfaces with several minima occur not infrequently" even for negative ions, which can undergo autodetachment [14].

[1] E. Teller and F. O. Rice, *The Structure of Matter* (John Wiley and Sons, New York, 1949), pp. 29, 247.

[2] P. P. Sutton and J. E. Mayer, J. Chem. Phys. **3**, 20 (1935).

[3] K. J. McCallum and J. E. Mayer, J. Chem. Phys. **11**, 56 (1943).

[4] P. M. Doty and J. E. Mayer, J. Chem. Phys. **12**, 323 (1944).

[5] F. M. Page and G. C. Goode, *Negative Ions and the Magnetron* (Wiley-Interscience, New York, 1969).

[6] E. C. M. Chen and E. S. Chen, *The Electron Capture Detector and The Study of Reactions with Thermal Electrons* (John Wiley and Sons, New York, 2004).

[7] L. G. Christophorou and J. K. Olthoff, *Fundamental Electron Interactions with Plasma Processing Gases* (Kluwer Academic/Plenum, New York, 2004).

[8] National Institute of Standards and Technology (NIST) Chemistry WebBook, 2005; http://webbook.nist.gov/

[9] J. E. Lovelock, Nature (London) **189**, 729. (1961).

[10] W. E. Wentworth, E. C. M. Chen, and J. E. Lovelock, J. Phys. Chem. **70**, 445 (1966).

[11] D. R. Herschbach, Angew. Chem., Int. Ed. Engl. **26**, 1221 (1987). This acronym was accepted by Professor Herschbach, after noting he simply followed W. B. Person.

[12] R. S. Mulliken, J. Chem. Phys. **33**, 247 (1960).

[13] E. C. M. Chen and E. S. Chen, J. Chromatogr. A **1037**, 83 (2004).

[14] E. C. M. Chen, C. Herder, C. Chang, R. Ting, and E. S. Chen, J. Phys. B **39**, 2317 (2006).

[15] E. C. M. Chen and E. S. Chen, Chem. Phys. Lett. **435**, 331 (2007).

[16] E. C. M. Chen, C. Herder, and E. S. Chen, Chem. Phys. Lett. **440**, 180 (2007).

[17] D. H. Paik, J. S. Baskin, N. J. Kim, and A. H. Zewail, J. Chem. Phys. **125**, 133408 (2006).

[18] W. M. Hickman and D. Berg, J. Chem. Phys. **29**, 517 (1958).

[19] E. C. M. Chen, R. D. George, and W. E. Wentworth, J. Chem. Phys. **49**, 1973 (1968).
[20] F. C. Fehsenfeld, J. Chem. Phys. **53**, 2000 (1970).
[21] C. L. Chen and P. J. Chantry, J. Chem. Phys. **71**, 3897 (1979).
[22] K. M. A. Refaey and J. L. Franklin, Int. J. Mass Spectrom. Ion Phys. **26**, 125 (1978).
[23] E. P. Grimsrud, S. Chowdhury, and P. J. Kebarle, Chem. Phys. **83**, 1059 (1985).
[24] R. S. Mock and E. P. Grimsrud, Chem. Phys. Lett. **184**, 99 (1991).
[25] P. G. Datskos, J. G. Carter, and L. G. Christophorou, Chem. Phys. Lett. **239**, 38 (1995).
[26] J. Kay and F. M. Page, Trans. Faraday Soc. **60**, 1042 (1964).
[27] A. C. Malliaris, J. Appl. Phys. **39**, 3675 (1968).
[28] D. Spence and G. J. Schultz, J. Chem. Phys. **58**, 3897 (1973).
[29] V. H. Shui, P. I. Singh, B. Kivel, and E. R. Bresselt, AIAA J. **17**, 1178 (1979).
[30] D. Smith, N. G. Adams, and E. Alge, J. Phys. B **17**, 461 (1984).
[31] J. L. Le Garrec, O. Sidko, J. L. Queffelec, S. Hamon, J. B. A. Mitchell, and B. R. Rowe, J. Chem. Phys. **107**, 54 (1997).
[32] E. C. M. Chen, L. R. Shuie, E. D. D'Sa, C. F. Batten, and W. E. Wentworth, J. Chem. Phys. **88**, 4711 (1988).
[33] E. C. M. Chen, J. R. Wiley, C. F. Batten, and W. E. Wentworth, J. Phys. Chem. **98**, 88 (1994).
[34] Lih Ren Shuie, Doctoral dissertation, University of Houston, 1984 (unpublished).
[35] Eia D. D'sa, Doctoral dissertation, University of Houston, 1987 (unpublished).
[36] E. A. Stemmler and R. A. Hites, *Electron Capture Negative Ion Mass Spectra of Environmental Contaminants and Related Compounds* (VCH, New York, 1988).
[37] W. E. Wentworth, W. Hirsch, and E. C. M. Chen, J. Phys. Chem. **71**, 218 (1967).
[38] H. S. W. Massey, *Negative Ions* (Cambridge University Press, New York, 1976), and earlier editions.
[39] H. O. Pritchard, Chem. Rev. (Washington, D.C.) **52**, 529 (1953).
[40] A. S. Streitweiser, *Molecular Orbital Theory for Organic Chemists* (Wiley, New York, 1961).
[41] G. Breigleb, Angew. Chem., Int. Ed. Engl. **617**, 1027 (1964).
[42] A. A. Christodoulides, D. L. McCorkle, and L. G. Christophorou, Electron Affinities of Atoms, Molecules and Radicals, in *Electron-Molecule Interactions and their Applications*, edited by L. G. Christophorou (Academic Press, New York, 1984).
[43] J. G. Dillard, Chem. Rev. (Washington, D.C.) **73**, 700 (1973).
[44] P. Kebarle and S. Chowdhury, Chem. Rev. (Washington, D.C.) **87**, 513 (1987).
[45] A. W. Kleyn and A. M. C. Moutinho, J. Phys. B **34**, R1 (2001).
[46] J. C. Rienstra-Kiracofe, G. S. Tschumper, H. F. Schaefer, III, S. Nandi, and G. B. Ellison, Chem. Rev. (Washington, D.C.) **102**, 231 (2002).
[47] E. C. M. Chen and W. E. Wentworth, Mol. Cryst. Liq. Cryst. **171**, 271 (1989).
[48] E. S. Chen, E. C. M. Chen, N. Sane, L. Talley, N. Kozanecki, and S. Schulze, J. Chem. Phys. **110**, 9319 (1999).
[49] E. S. Chen, E. C. M. Chen, N. Sane, and S. Schulze, Bioelectrochem. Bioenerg. **48**, 69 (1999).
[50] S. Steenken, J. P. Telo, H. M. Novais, and L. P. Candeias, J. Am. Chem. Soc. **114**, 4701 (1992).
[51] G. Herzberg, *Molecular Spectra and Molecular Structure* (D. Van Nostrand Company, Princeton, New Jersey, 1967).